Supplementary Information of Proton transfer in the hydrogen-bond chains of lepidocrocite: A computational study

Haibo Guo[*a] **and Amanda S. Barnard**[a]

Received Xth XXXXXXXXXX 20XX, Accepted Xth XXXXXXXXX 20XX
First published on the web Xth XXXXXXXXXX 200X
DOI: 10.1039/b000000x

1 Computational methodology and settings

In our density functional theory (DFT) calculations, the Kohn-Sham one-electron states were expanded using plane-wave basis sets. Our convergence tests showed a plane-wave cut-off of 500 eV is sufficient to converge the calculated energies to 2 meV/atom. The Buillouin zone is sampled using the Monkhorst-Pack scheme[1] with an $11 \times 11 \times 9$ mesh for the primitive cell (containing 2 FeOOH formula) or a $9 \times 3 \times 7$ mesh for the base-centred convention cell (containing 4 FeOOH formula). The numbers of irreducible *k*-points in the first Brillouin zone are 180 for the primitive cell and 40 for the convention cell. The convergence criterion for self-consistent electronic iterations was 0.5×10^{-5} eV. Geometry optimizations were performed using the conjugate gradient algorithm until the residual forces were smaller than 0.005 eV/Å.

In order to reduce the noise in the calculated forces, we have used a tighter criterion of 1.0×10^{-8} eV for the electronic iterations, and re-optimize the crystal structure to reduce the residue force to below 0.2 meV/Å. In the phonon calculations we have elected to evaluate the projection operators in reciprocal space to improve the accuracy. We found small imaginary acoustic frequencies ($\sim 10\,\mathrm{cm}^{-1}$) in the breathing mode (ZA) persisted in all the tested super cells due to numerical errors. It has been previously shown that such noise can be safely removed using an extrapolation method.[2]

As mentioned in the main texts, we have used the climbing image nudged elastic band (CI–NEB) method to search for the transition states of proton transfer and the energy barrier.[3,4] The CI–NEB method enables the states close to extrema to be promoted to the extrema to find the saddle points, which significantly improves the convergence speed compared to other NEB methods. We have tested the convergence of the energy barrier with respect to the number of images (up to 20), and selected to use 16 images to locate the saddle points. We have used the BFGS (Broyden-Fletcher-Goldfarb-Shanno) optimizer of the VTST code[5] to find the minimum energy transition path. In searching for the transition path and calculating the energy barrier, We allowed all the atoms in the system to relax.

2 Electronic structure

Lepidocrocite is a semiconductor with a small band gap of 2.06 eV.[6] This strongly correlated material was poorly described in our DFT calculations using the PBE functionals. As we see from Fig. 1 that the PBE functionals incorrectly predict lepidocrocite is metallic with appreciable electronic states at the Fermi level. In contrast, the GGA+U (with $U_{\mathrm{eff}} = 4.5$ eV) opens up the Kohn-Sham one-electron band gap to ~ 1.7 eV and reproduces the semiconducting feature of lepidocrocite.

The parameter U has been tested with five iron oxides and oxyhydroxides to reproduce the experimental lattice parameters.[7] The ideal way to obtain this parameter is through the linear response method that is internally consistent with the rest of *ab initio* calculations.[8] However, it is frequently treated as an adjustable parameter which is tuned for different systems and applications. The DFT+U method has previously been employed to study magnetite[9,10], hematite[11–13], goethite[14], and maghemite[15], for which the parameter U varies between 2 eV to 5 eV. The U parameter used in our calculations (4.5 eV) is within the range of these reported values.

3 Crystal structure

The optimized lattice parameters by GGA+U are listed in Table 1 together with experimental values from the literature. While the calculated a and b agree well with most experimental measurements, the c is slightly overestimated by 1.7%, which is expected because both GGA and on-site Coulomb interactions would overestimate lattice parameters. Since the b-axis is perpendicular to the double-sheet layers which are held

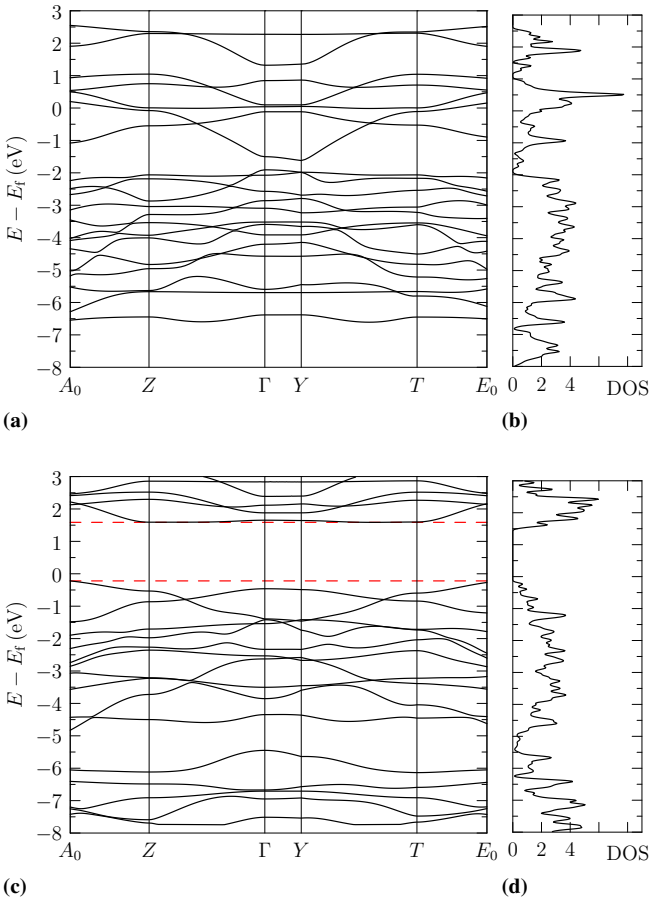

Fig. 1 Electronic band structure along high-symmetry lines and density of states of lepidocrocite. The parameter U_{eff} is 0 eV (i.e. no on-site Coulomb interaction) in calculating the band structure (a) and DOS (b); and $U_{\text{eff}} = 4.5$ eV for (c) and (d).

by hydrogen bonds, the small variation of the experimental measurements (from 12.49 to 12.54 Å) may reflect to the variation of inter-layer distances, or bond lengths of the hydrogen bonds, in different samples with different levels of defects. The *b* lattice parameter in our calculations reside in the range of (available) experimental measurements, indicating the description of the hydrogen bonds by the GGA+U method is adequate.

In addition to this, the calculated atomic positions of Fe and O compare well with those measured using electron diffraction (ED, in Ref.[19]) and neutron diffraction (ND, in Ref.[18]), as shown in Table 2. The difference in z-components of the atomic coordinates arise from the choices of symmetry groups. Our calculations and the measurements using ND are based on the space group $Cmc2_1$ (No. 36) where the z-components of positions 4*a* and 8*b* are not fixed, while the measurements using ED are based on the space group Cmcm (No. 63) where the z-components of positions 4*c* and 8*f* are fixed (= 1/4). The atomic positions of hydrogen atoms in the optimized structure are different in the two data sets, but the differences in the coordinates of Fe and O are very small. If hydrogen atoms were omitted, both space groups would describe well the crystal structure of lepidocrocite. The positions of hydrogen atoms are therefore decisive in distinguishing between the two symmetry groups.

Determining the positions of the hydrogen atoms turned out to be difficult. The electron cloud of hydrogen atoms diffracts x-ray weakly, and the hydrogen atoms tend to be mobile as they vibrate at high frequencies (compared with heavier elements) or change their positions frequently. Researchers have identified using ND and ED the time- and space-averaged positions of hydrogen atoms, which are compatible with the Cmcm symmetry.[16–19] However, the centered O–H–O hydrogen bond in this symmetry has abnormally large bond length, and it is more likely the hydrogen bonds are asymmetric and the crystal symmetry is $Cmc2_1$.[18]

As shown in the main text, a hydrogen atom frequently switches between the two stable positions in a O–H···O bond, and the time-averaged effect is a centred O–H–O bond and the Cmcm symmetry. Even when this vibration was quenched, the Cmcm symmetry should persist because of the structural disorder of coexisting energy-degenerate configurations of the hydrogen-bond chains. These coexisting configurations give rise to the pseudo-symmetry of Cmcm. Our results confirm that the short-distance displacements of hydrogen atoms and the energy-degenerate configurations of the hydroxyl groups are the sources of difficulties in the structural characterization.

References

1 H. J. Monkhorst and J. D. Pack, *Phys. Rev. B*, 1976, **13**, 5188–5192.
2 K. A. Velizhanin, S. Kilina, T. D. Sewell and A. Piryatinski, *J. Phys. Chem. B*, 2008, **112**, 13252–13257.
3 G. Henkelman, B. P. Uberuaga and H. Jóosson, *J. Chem. Phys.*, 2000, **113**, 9901–9904.
4 H. Jónsson, G. Mills and K. W. Jacobsen, *Classical and Quantum Dynamics in Condensed Phase Simulations*, World Scientific, Singapore, 1998, ch. 16, p. 385.
5 D. Sheppard, R. Terrell and G. Henkelman, *J. Chem. Phys.*, 2008, **128**, 134106.
6 R. M. Cornell and U. Schwertmann, *The iron oxides*, Wiley-VCH, Weinheim, Germany, 2nd edn, 2003.
7 H. B. Guo and A. S. Barnard, *Phys. Rev. B*, 2011, **83**, 094112.
8 M. Cococcioni and S. de Gironcoli, *Phys. Rev. B*, 2005, **71**, 035105.
9 G. K. H. Madsen and P. Novák, *Europhys. Lett.*, 2005, **69**, 777–783.
10 Z. Zhang and S. Satpathy, *Phys. Rev. B*, 1991, **44**, 13319–13331.
11 M. P. J. Punkkinen, K. Kokko, W. Hergert and I. J. Väyrynen, *J. Phys.: Condens. Matter*, 1999, **11**, 2341–2349.
12 G. Rollmann, A. Rohrbach, P. Entel and J. Hafner, *Phys. Rev. B*, 2004, **69**, 165107.
13 A. Rohrbach, J. Hafner and G. Kresse, *Phys. Rev. B*, 2004, **70**, 125426.
14 B. Russell, M. Payne and L. C. Ciacchi, *Phys. Rev. B*, 2009, **79**, 165101.

Table 1 Lattice parameters of lepidocrocite from GGA+U calculations and from the literature.

a (Å)	b (Å)	c (Å)	Technique	Sample	Ref.
3.074	12.564	3.936	GGA+U	-	This work
3.06	12.51	3.87	XRD	Natural	[16]
3.36	12.49	3.86	XRD	Synthetic	[17]
3.08	12.50	3.87	ND	Synthetic & Natural	[18]
3.072	12.516	3.873	ED	Synthetic	[19]
3.063∼3.068	12.521∼12.539	3.866∼3.870	XRD	Synthetic	[20]

Table 2 Calculated and measured atomic positions in lepidocrocite. The coordinates are fractional with respect to the convention cell. O(1) refers to those oxygen atoms that form bonds with Fe only, and O(2) refers to the oxygen atoms that form hydroxyl bonds.

	GGA+U	ED.[19]	ND.[18]
Fe	(0.5, 0.1766, 0.2579)	(0.5, 0.1778, 0.25)	(0.5, 0.177, 0.25)
H	(0, 0.0181, 0.4481)	(0, -0.001, 0.179)	(0, 0.025, 0.452)
O(1)	(0, 0.2885, 0.2581)	(0, 0.2889, 0.25)	(0, 0.295, 0.266)
O(2)	(0, 0.0709, 0.2539)	(0, 0.0738, 0.25)	(0, 0.072, 0.250)

15 R. Grau-Crespo, A. Y. Al-Baitai, I. Saadoune and N. H. de Leeuw, *J. Phys.: Condens. Matter*, 2010, **22**, 255401.
16 E. J. Ewing, *J. Chem. Phys.*, 1935, **3**, 420–424.
17 A. Y. Vlasov, N. A. Gornushkina and M. I. Petrov, *Izvestiya Vysshikh Zavedenii, Fizika*, 1972, **5**, 84–90.
18 H. Christensen and A. N. Christensen, *Acta Chem. Scand. A*, 1978, **32**, 87–88.
19 A. P. Zhukhlistov, *Crystallogr Rep*, 2001, **46**, 730–733.
20 J. Majzlan, L. Mazeina and A. Navrotsky, *Geochemica et Cosmochimica Acta*, 2007, **71**, 615–623.